Search for the decay $D_s^+ \to p\bar{p}e^+\nu_e$

M. Ablikim,[1] M. N. Achasov,[10,e] P. Adlarson,[63] S. Ahmed,[15] M. Albrecht,[4] A. Amoroso,[62a,62c] Q. An,[59,47] Anita,[21] Y. Bai,[46] O. Bakina,[28] R. Baldini Ferroli,[23a] I. Balossino,[24a] Y. Ban,[37,l] K. Begzsuren,[26] J. V. Bennett,[5] N. Berger,[27] M. Bertani,[23a] D. Bettoni,[24a] F. Bianchi,[62a,62c] J. Biernat,[63] J. Bloms,[56] A. Bortone,[62a,62c] I. Boyko,[28] R. A. Briere,[5] H. Cai,[64] X. Cai,[1,47] A. Calcaterra,[23a] G. F. Cao,[1,51] N. Cao,[1,51] S. A. Cetin,[50b] J. F. Chang,[1,47] W. L. Chang,[1,51] G. Chelkov,[28,c,d] D. Y. Chen,[6] G. Chen,[1] H. S. Chen,[1,51] M. L. Chen,[1,47] S. J. Chen,[35] X. R. Chen,[25] Y. B. Chen,[1,47] W. Cheng,[62c] G. Cibinetto,[24a] F. Cossio,[62c] X. F. Cui,[36] H. L. Dai,[1,47] J. P. Dai,[41,i] X. C. Dai,[1,51] A. Dbeyssi,[15] R. B. de Boer,[4] D. Dedovich,[28] Z. Y. Deng,[1] A. Denig,[27] I. Denysenko,[28] M. Destefanis,[62a,62c] F. De Mori,[62a,62c] Y. Ding,[33] C. Dong,[36] J. Dong,[1,47] L. Y. Dong,[1,51] M. Y. Dong,[1,47,51] S. X. Du,[67] J. Fang,[1,47] S. S. Fang,[1,51] Y. Fang,[1] R. Farinelli,[24a,24b] L. Fava,[62b,62c] F. Feldbauer,[4] G. Felici,[23a] C. Q. Feng,[59,47] M. Fritsch,[4] C. D. Fu,[1] Y. Fu,[1] X. L. Gao,[59,47] Y. Gao,[60] Y. Gao,[37,l] Y. G. Gao,[6] I. Garzia,[24a,24b] E. M. Gersabeck,[54] A. Gilman,[55] K. Goetzen,[11] L. Gong,[36] W. X. Gong,[1,47] W. Gradl,[27] M. Greco,[62a,62c] L. M. Gu,[35] M. H. Gu,[1,47] S. Gu,[2] Y. T. Gu,[13] C. Y. Guan,[1,51] A. Q. Guo,[22] L. B. Guo,[34] R. P. Guo,[39] Y. P. Guo,[27] A. Guskov,[28] S. Han,[64] T. T. Han,[40] T. Z. Han,[9,j] X. Q. Hao,[16] F. A. Harris,[52] K. L. He,[1,51] F. H. Heinsius,[4] T. Held,[4] Y. K. Heng,[1,47,51] M. Himmelreich,[11,h] T. Holtmann,[4] Y. R. Hou,[51] Z. L. Hou,[1] H. M. Hu,[1,51] J. F. Hu,[41,i] T. Hu,[1,47,51] Y. Hu,[1] G. S. Huang,[59,47] L. Q. Huang,[60] X. T. Huang,[40] N. Huesken,[56] T. Hussain,[61] W. Ikegami,[63] W. Imoehl Andersson,[22] M. Irshad,[59,47] S. Jaeger,[4] Q. Ji,[1] Q. P. Ji,[16] X. B. Ji,[1,51] X. L. Ji,[1,47] H. B. Jiang,[40] X. S. Jiang,[1,47,51] X. Y. Jiang,[36] J. B. Jiao,[40] Z. Jiao,[18] S. Jin,[35] Y. Jin,[53] T. Johansson,[63] N. Kalantar-Nayestanaki,[30] X. S. Kang,[33] R. Kappert,[30] M. Kavatsyuk,[30] B. C. Ke,[42,1] I. K. Keshk,[4] A. Khoukaz,[56] P. Kiese,[27] R. Kiuchi,[1] R. Kliemt,[11] L. Koch,[29] O. B. Kolcu,[50b,g] B. Kopf,[4] M. Kuemmel,[4] M. Kuessner,[4] A. Kupsc,[63] M. G. Kurth,[1,51] W. Kühn,[29] J. J. Lane,[54] J. S. Lange,[29] P. Larin,[15] L. Lavezzi,[62c] H. Leithoff,[27] M. Lellmann,[27] T. Lenz,[27] C. Li,[38] C. H. Li,[32] Cheng Li,[59,47] D. M. Li,[67] F. Li,[1,47] G. Li,[1] H. B. Li,[1,51] H. J. Li,[9,j] J. L. Li,[40] Ke Li,[1] L. K. Li,[1] Lei Li,[3] P. L. Li,[59,47] P. R. Li,[31] W. D. Li,[1,51] W. G. Li,[1] X. H. Li,[59,47] X. L. Li,[40] Z. B. Li,[48] Z. Y. Li,[48] H. Liang,[1,51] H. Liang,[59,47] Y. F. Liang,[44] Y. T. Liang,[25] L. Z. Liao,[1,51] J. Libby,[21] C. X. Lin,[48] D. X. Lin,[15] B. Liu,[41,i] B. J. Liu,[1] C. X. Liu,[1] D. Liu,[59,47] D. Y. Liu,[41,i] F. H. Liu,[43] Fang Liu,[1] Feng Liu,[6] H. B. Liu,[13] H. M. Liu,[1,51] Huanhuan Liu,[1] Huihui Liu,[17] J. B. Liu,[59,47] J. Y. Liu,[1,51] K. Liu,[1] K. Y. Liu,[33] Ke Liu,[6] L. Liu,[59,47] L. Y. Liu,[13] Q. Liu,[51] S. B. Liu,[59,47] T. Liu,[1,51] X. Liu,[31] Y. B. Liu,[36] Z. A. Liu,[1,47,51] Zhiqing Liu,[40] Y. F. Long,[37,l] X. C. Lou,[1,47,51] H. J. Lu,[18] J. D. Lu,[1,51] J. G. Lu,[1,47] X. L. Lu,[1] Y. Lu,[1] Y. P. Lu,[1,47] C. L. Luo,[34] M. X. Luo,[66] P. W. Luo,[48] T. Luo,[9,j] X. L. Luo,[1,47] S. Lusso,[62c] X. R. Lyu,[51] F. C. Ma,[33] H. L. Ma,[1] L. L. Ma,[40] M. M. Ma,[1,51] Q. M. Ma,[1] R. Q. Ma,[1,51] R. T. Ma,[51] X. N. Ma,[36] X. X. Ma,[1,51] X. Y. Ma,[1,47] Y. M. Ma,[40] F. E. Maas,[15] M. Maggiora,[62a,62c] S. Maldaner,[27] S. Malde,[57] Q. A. Malik,[61] A. Mangoni,[23b] Y. J. Mao,[37,l] Z. P. Mao,[1] S. Marcello,[62a,62c] Z. X. Meng,[53] J. G. Messchendorp,[30] G. Mezzadri,[24a] T. J. Min,[35] R. E. Mitchell,[22] X. H. Mo,[1,47,51] Y. J. Mo,[6] C. Morales,[15] N. Yu. Muchnoi Morales,[10,e] H. Muramatsu,[55] S. Nakhoul,[11,h] Y. Nefedov,[28] F. Nerling,[11,h] I. B. Nikolaev,[10,e] Z. Ning,[1,47] S. Nisar,[8,k] S. L. Olsen,[51] Q. Ouyang,[1,47,51] S. Pacetti,[23b] Y. Pan,[54] Y. Pan,[59,47] M. Papenbrock,[63] A. Pathak,[1] P. Patteri,[23a] M. Pelizaeus,[4] H. P. Peng,[59,47] K. Peters,[11,h] J. Pettersson,[63] J. L. Ping,[34] R. G. Ping,[1,51] A. Pitka,[4] R. Poling,[55] V. Prasad,[59,47] H. Qi,[59,47] M. Qi,[35] S. Qian,[1,47] C. F. Qiao,[51] L. Q. Qin,[12] X. P. Qin,[13] X. S. Qin,[4] Z. H. Qin,[1,47] J. F. Qiu,[1] S. Q. Qu,[36] K. H. Rashid,[61] K. Ravindran,[21] C. F. Redmer,[27] M. Richter,[4] A. Rivetti,[62c] V. Rodin,[30] M. Rolo,[62c] G. Rong,[1,51] Ch. Rosner,[15] M. Rump,[56] A. Sarantsev,[28,f] M. Savrié,[24b] Y. Schelhaas,[27] C. Schnier,[4] K. Schoenning,[63] W. Shan,[19] X. Y. Shan,[59,47] M. Shao,[59,47] C. P. Shen,[2] P. X. Shen,[36] X. Y. Shen,[1,51] H. C. Shi,[59,47] R. S. Shi,[1,51] X. Shi,[1,47] X. D. Shi,[59,47] J. J. Song,[40] Q. Q. Song,[59,47] Y. X. Song,[37,l] S. Sosio,[62a,62c] C. Sowa,[4] S. Spataro,[62a,62c] F. F. Sui,[40] G. X. Sun,[1] J. F. Sun,[16] L. Sun,[64] S. S. Sun,[1,51] T. Sun,[1,51] W. Y. Sun,[34] Y. J. Sun,[59,47] Y. K. Sun,[59,47] Y. Z. Sun,[1] Z. T. Sun,[1] Y. X. Tan,[59,47] C. J. Tang,[44] G. Y. Tang,[1] V. Thoren,[63] B. Tsednee,[26] I. Uman,[50d] B. Wang,[1] B. L. Wang,[51] C. W. Wang,[35] D. Y. Wang,[37,l] H. P. Wang,[1,51] K. Wang,[1,47] L. L. Wang,[1] M. Wang,[40] M. Z. Wang,[37,l] Meng Wang,[1,51] W. P. Wang,[59,47] X. Wang,[37,l] X. F. Wang,[31] X. L. Wang,[9,j] Y. Wang,[48] Y. Wang,[59,47] Y. D. Wang,[15] Y. F. Wang,[1,47,51] Y. Q. Wang,[1] Z. Wang,[1,47] Z. Y. Wang,[1] Ziyi Wang,[51] Zongyuan Wang,[1,51] T. Weber,[4] D. H. Wei,[12] P. Weidenkaff,[27] F. Weidner,[56] H. W. Wen,[34,a] S. P. Wen,[1] D. J. White,[54] U. Wiedner,[4] G. Wilkinson,[57] M. Wolke,[63] L. Wollenberg,[4] J. F. Wu,[1,51] L. H. Wu,[1] L. J. Wu,[1,51] Z. Wu,[1,47] L. Xia,[59,47] S. Y. Xiao,[1] Y. J. Xiao,[1,51] Z. J. Xiao,[34] Y. G. Xie,[1,47] Y. H. Xie,[6] T. Y. Xing,[1,51] X. A. Xiong,[1,51] G. F. Xu,[1] J. J. Xu,[35] Q. J. Xu,[14] W. Xu,[1,51] X. P. Xu,[45] L. Yan,[62a,62c] W. B. Yan,[59,47] W. C. Yan,[2] H. J. Yang,[41,i] H. X. Yang,[1] L. Yang,[64] R. X. Yang,[59,47] S. L. Yang,[1,51] Y. H. Yang,[35] Y. X. Yang,[12] Yifan Yang,[1,51] Zhi Yang,[25] M. Ye,[1,47] M. H. Ye,[7] J. H. Yin,[1] Z. Y. You,[48] B. X. Yu,[1,47,51] C. X. Yu,[36] G. Yu,[1,51] J. S. Yu,[20] T. Yu,[60] C. Z. Yuan,[1,51] W. Yuan,[62a,62c] X. Q. Yuan,[37,l] Y. Yuan,[1] C. X. Yue,[32] A. Yuncu,[50b,b] A. A. Zafar,[61] Y. Zeng,[20] B. X. Zhang,[1] Guangyi Zhang,[16] H. H. Zhang,[48] H. Y. Zhang,[1,47] J. L. Zhang,[65] J. Q. Zhang,[4] J. W. Zhang,[1,47,51] J. Y. Zhang,[1] J. Z. Zhang,[1,51] Jianyu Zhang,[1,51] Jiawei Zhang,[1,51] L. Zhang,[1] Lei Zhang,[35] S. Zhang,[48] S. F. Zhang,[35] T. J. Zhang,[41,i] X. Y. Zhang,[40] Y. Zhang,[57] Y. H. Zhang,[1,47] Y. T. Zhang,[59,47] Yan Zhang,[59,47] Yao Zhang,[1] Yi Zhang,[9,j] Z. H. Zhang,[6] Z. Y. Zhang,[64] G. Zhao,[1] J. Zhao,[32] J. Y. Zhao,[1,51] J. Z. Zhao,[1,47] Lei Zhao,[59,47] Ling Zhao,[1] M. G. Zhao,[36]

Q. Zhao,[1] S. J. Zhao,[67] Y. B. Zhao,[1,47] Z. G. Zhao,[59,47] A. Zhemchugov,[28,c] B. Zheng,[60] J. P. Zheng,[1,47] Y. Zheng,[37,l] Y. H. Zheng,[51] B. Zhong,[34] C. Zhong,[60] L. P. Zhou,[1,51] Q. Zhou,[1,51] X. Zhou,[64] X. K. Zhou,[51] X. R. Zhou,[59,47] A. N. Zhu,[1,51] J. Zhu,[36] K. Zhu,[1] K. J. Zhu,[1,47,51] S. H. Zhu,[58] W. J. Zhu,[36] X. L. Zhu,[49] Y. C. Zhu,[59,47] Z. A. Zhu,[1,51] B. S. Zou,[1] and J. H. Zou[1]

(BESIII Collaboration)

[1]*Institute of High Energy Physics, Beijing 100049, People's Republic of China*
[2]*Beihang University, Beijing 100191, People's Republic of China*
[3]*Beijing Institute of Petrochemical Technology, Beijing 102617, People's Republic of China*
[4]*Bochum Ruhr-University, D-44780 Bochum, Germany*
[5]*Carnegie Mellon University, Pittsburgh, Pennsylvania 15213, USA*
[6]*Central China Normal University, Wuhan 430079, People's Republic of China*
[7]*China Center of Advanced Science and Technology, Beijing 100190, People's Republic of China*
[8]*COMSATS University Islamabad, Lahore Campus, Defence Road, Off Raiwind Road, 54000 Lahore, Pakistan*
[9]*Fudan University, Shanghai 200443, People's Republic of China*
[10]*G.I. Budker Institute of Nuclear Physics SB RAS (BINP), Novosibirsk 630090, Russia*
[11]*GSI Helmholtzcentre for Heavy Ion Research GmbH, D-64291 Darmstadt, Germany*
[12]*Guangxi Normal University, Guilin 541004, People's Republic of China*
[13]*Guangxi University, Nanning 530004, People's Republic of China*
[14]*Hangzhou Normal University, Hangzhou 310036, People's Republic of China*
[15]*Helmholtz Institute Mainz, Johann-Joachim-Becher-Weg 45, D-55099 Mainz, Germany*
[16]*Henan Normal University, Xinxiang 453007, People's Republic of China*
[17]*Henan University of Science and Technology, Luoyang 471003, People's Republic of China*
[18]*Huangshan College, Huangshan 245000, People's Republic of China*
[19]*Hunan Normal University, Changsha 410081, People's Republic of China*
[20]*Hunan University, Changsha 410082, People's Republic of China*
[21]*Indian Institute of Technology Madras, Chennai 600036, India*
[22]*Indiana University, Bloomington, Indiana 47405, USA*
[23a]*INFN Laboratori Nazionali di Frascati, I-00044 Frascati, Italy*
[23b]*INFN and University of Perugia, I-06100 Perugia, Italy*
[24a]*INFN Sezione di Ferrara, I-44122 Ferrara, Italy*
[24b]*University of Ferrara, I-44122 Ferrara, Italy*
[25]*Institute of Modern Physics, Lanzhou 730000, People's Republic of China*
[26]*Institute of Physics and Technology, Peace Avenue 54B, Ulaanbaatar 13330, Mongolia*
[27]*Johannes Gutenberg University of Mainz, Johann-Joachim-Becher-Weg 45, D-55099 Mainz, Germany*
[28]*Joint Institute for Nuclear Research, 141980 Dubna, Moscow Region, Russia*
[29]*Justus-Liebig-Universitaet Giessen, II. Physikalisches Institut, Heinrich-Buff-Ring 16, D-35392 Giessen, Germany*
[30]*KVI-CART, University of Groningen, NL-9747 AA Groningen, Netherlands*
[31]*Lanzhou University, Lanzhou 730000, People's Republic of China*
[32]*Liaoning Normal University, Dalian 116029, People's Republic of China*
[33]*Liaoning University, Shenyang 110036, People's Republic of China*
[34]*Nanjing Normal University, Nanjing 210023, People's Republic of China*
[35]*Nanjing University, Nanjing 210093, People's Republic of China*
[36]*Nankai University, Tianjin 300071, People's Republic of China*
[37]*Peking University, Beijing 100871, People's Republic of China*
[38]*Qufu Normal University, Qufu 273165, People's Republic of China*
[39]*Shandong Normal University, Jinan 250014, People's Republic of China*
[40]*Shandong University, Jinan 250100, People's Republic of China*
[41]*Shanghai Jiao Tong University, Shanghai 200240, People's Republic of China*
[42]*Shanxi Normal University, Linfen 041004, People's Republic of China*
[43]*Shanxi University, Taiyuan 030006, People's Republic of China*
[44]*Sichuan University, Chengdu 610064, People's Republic of China*
[45]*Soochow University, Suzhou 215006, People's Republic of China*
[46]*Southeast University, Nanjing 211100, People's Republic of China*
[47]*State Key Laboratory of Particle Detection and Electronics, Beijing 100049, Hefei 230026, People's Republic of China*

[48]Sun Yat-Sen University, Guangzhou 510275, People's Republic of China
[49]Tsinghua University, Beijing 100084, People's Republic of China
[50a]Ankara University, 06100 Tandogan, Ankara, Turkey
[50b]Istanbul Bilgi University, 34060 Eyup, Istanbul, Turkey
[50c]Uludag University, 16059 Bursa, Turkey
[50d]Near East University, Nicosia, North Cyprus, Mersin 10, Turkey
[51]University of Chinese Academy of Sciences, Beijing 100049, People's Republic of China
[52]University of Hawaii, Honolulu, Hawaii 96822, USA
[53]University of Jinan, Jinan 250022, People's Republic of China
[54]University of Manchester, Oxford Road, Manchester M13 9PL, United Kingdom
[55]University of Minnesota, Minneapolis, Minnesota 55455, USA
[56]University of Muenster, Wilhelm-Klemm-Straße 9, 48149 Muenster, Germany
[57]University of Oxford, Keble Road, Oxford, United Kingdom OX13RH
[58]University of Science and Technology Liaoning, Anshan 114051, People's Republic of China
[59]University of Science and Technology of China, Hefei 230026, People's Republic of China
[60]University of South China, Hengyang 421001, People's Republic of China
[61]University of the Punjab, Lahore-54590, Pakistan
[62a]University of Turin, I-10125 Turin, Italy
[62b]University of Eastern Piedmont, I-15121 Alessandria, Italy
[62c]INFN, I-10125 Turin, Italy
[63]Uppsala University, Box 516, SE-75120 Uppsala, Sweden
[64]Wuhan University, Wuhan 430072, People's Republic of China
[65]Xinyang Normal University, Xinyang 464000, People's Republic of China
[66]Zhejiang University, Hangzhou 310027, People's Republic of China
[67]Zhengzhou University, Zhengzhou 450001, People's Republic of China

(Received 29 October 2019; published 24 December 2019)

Using a 3.19 fb^{-1} data sample collected at the $\sqrt{s} = 4.178$ GeV with the BESIII detector, we search for the rare decay $D_s^+ \to p\bar{p}e^+\nu_e$. No significant signal is observed, and an upper limit of $\mathcal{B}(D_s^+ \to p\bar{p}e^+\nu_e) < 2.0 \times 10^{-4}$ is set at the 90% confidence level. This measurement is useful input in understanding the baryonic transition of D_s^+ mesons.

DOI: 10.1103/PhysRevD.100.112008

I. INTRODUCTION

In the charm sector, probing the transition between charm meson and baryon pairs is still largely an unexplored territory. Phase-space constraints dictate that only the D_s^+ meson can decay in such a manner. Until now, only one baryonic mode, $D_s^+ \to p\bar{n}$, has been observed. It was first seen by the CLEO Collaboration, with a branching fraction of $(1.30 \pm 0.4) \times 10^{-3}$ [1], and subsequently confirmed by

[a]Also at Ankara University, 06100 Tandogan, Ankara, Turkey.
[b]Also at Bogazici University, 34342 Istanbul, Turkey.
[c]Also at the Moscow Institute of Physics and Technology, Moscow 141700, Russia.
[d]Also at the Functional Electronics Laboratory, Tomsk State University, Tomsk 634050, Russia.
[e]Also at the Novosibirsk State University, Novosibirsk 630090, Russia.
[f]Also at the NRC "Kurchatov Institute," PNPI, 188300 Gatchina, Russia.
[g]Also at Istanbul Arel University, 34295 Istanbul, Turkey.
[h]Also at Goethe University Frankfurt, 60323 Frankfurt am Main, Germany.
[i]Also at Key Laboratory for Particle Physics, Astrophysics and Cosmology, Ministry of Education; Shanghai Key Laboratory for Particle Physics and Cosmology; Institute of Nuclear and Particle Physics, Shanghai 200240, People's Republic of China.
[j]Also at Key Laboratory of Nuclear Physics and Ion-beam Application (MOE) and Institute of Modern Physics, Fudan University, Shanghai 200443, People's Republic of China.
[k]Also at Harvard University, Department of Physics, Cambridge, MA, 02138, USA.
[l]Also at State Key Laboratory of Nuclear Physics and Technology, Peking University, Beijing 100871, People's Republic of China School of Physics and Electronics, Hunan University, Changsha 410082, China.

BESIII [2]. This mode is expected to be suppressed by chiral symmetry, and predictions for its decay rate are several orders of magnitude below the observed value [3], motivating the study of other baryonic channels. A promising candidate is the semileptonic decay mode $D_s^+ \to p\bar{p}e^+\nu_e$, for which theoretical calculations are expected to be more robust. Recently, Cheng and Kang [4] predicted a small branching fraction, $\mathcal{B}(D_s^+ \to p\bar{p}e^+\nu_e) \sim 10^{-8}$. Even in this case, however, there are significant uncertainties on the prediction, associated with the challenge of calculating the hadronic form factor. Experimental input is therefore needed to help illuminate this poorly understood class of charm decays.

An additional motivation for searching for this decay is that the final state provides an ideal laboratory to study the near-threshold enhancement phenomenon. This behavior was initially observed in the radiative process $J/\psi \to \gamma p\bar{p}$ by BESIII [5] and confirmed by CLEO [6] and BESIII [7], but not yet observed in other processes [8–10]. A very attractive feature of searching for this phenomenon in $D_s^+ \to p\bar{p}e^+\nu_e$ decays is that the $p\bar{p}$ system is produced close to the mass threshold.

With the strong interaction dynamics described by a form factor $f_+(q^2)$, and in the limit of zero electron mass, the differential rate for the $D_s^+ \to p\bar{p}e^+\nu_e$ decay is given by

$$\frac{d\Gamma(D_s^+ \to Xe^+\nu_e)}{dq^2} = \frac{G_F^2|V_{cs}|^2}{24\pi^3} p_X^3 |f_+(q^2)|^2, \quad (1)$$

where G_F is the Fermi constant; V_{cs} is the Cabibbo-Kobayashi-Maskawa (CKM) matrix element; the X represents the $p\bar{p}$ system, which is assumed to form a $^1S_0$ state; p_X is the momentum of the $p\bar{p}$ system in the rest frame of the D_s^+ meson; and q is the transition momentum between X and D_s^+. The form factor $f_+(q^2)$ is described by the well-known ISGW2 model [11],

$$f_+(q^2) = f_+(q^2_{\rm max})\left(1 + \frac{r^2}{12}(q^2_{\rm max} - q^2)\right)^{-1}, \quad (2)$$

where r is the effective radius of the D_s^+ meson, and $q^2_{\rm max}$ is the kinematic limit of q^2.

In this article, we report a search for the decay $D_s^+ \to p\bar{p}e^+\nu_e$ using a 3.19 fb^{-1} data set collected at $\sqrt{s} =$ 4.178 GeV with the BESIII detector operating at the BEPCII collider.

II. BESIII DETECTOR AND MONTE CARLO SIMULATION

The BESIII detector is a magnetic spectrometer [12] located at the Beijing Electron Position Collider (BEPCII) [13]. The cylindrical core of the BESIII detector consists of a helium-based multilayer drift chamber (MDC), a plastic scintillator time-of-flight system (TOF), and a CsI (Tl) electromagnetic calorimeter (EMC), which are all enclosed in a superconducting solenoidal magnet providing a 1.0 T magnetic field. The solenoid is supported by an octagonal flux-return yoke with resistive-plate counter muon-identifier modules interleaved with steel. The acceptance of charged particles and photons is 93% over the 4π solid angle. The charged-particle momentum resolution at 1 GeV/c is 0.5%, and the dE/dx resolution is 6% for the electrons from Bhabha scattering. The EMC measures photon energies with a resolution of 2.5% (5%) at 1 GeV in the barrel (end-cap) region. The time resolution of the TOF barrel part is 68 ps. The end-cap TOF system was upgraded in 2015 with multigap resistive plate chamber technology, providing a time resolution of 60 ps [14,15].

Simulated events are generated with a GEANT4-based [16] software package using a detailed description of the detector geometry and of the particle interactions in the detector material. A sample of inclusive Monte Carlo (MC) simulation is produced at $\sqrt{s} = 4.178$ GeV. This sample includes all known open-charm decay processes and the $c\bar{c}$ resonances, J/ψ, $\psi(3686)$, and $\psi(3770)$ via the initial state radiation (ISR). Additionally, the continuum process ($e^+e^- \to q\bar{q}$, $q = u$, d, and s), Bhabha scattering, $\mu^+\mu^-$, $\tau^+\tau^-$, as well as two-photon process are included. The open charm processes are generated using CONEXC [17] and their subsequent decays are modeled by EVTGEN [18] with the known branching fractions from the Particle Data Group [19], and the remaining unknown decay modes of the narrow $c\bar{c}$ resonances are generated using the modified LUND model [20]. The signal model is described by Eq. (1). We assume that the $p\bar{p}$ S-wave system dominates in the decay and adopt a nonresonance S-wave to describe the $p\bar{p}$ system (when assigning the systematic uncertainties we also consider the possibility of a resonance contributing to the decay).

III. ANALYSIS METHOD

Throughout the paper, charge-conjugate modes are implicitly implied, unless otherwise noted. The $D_s^\pm D_s^{*\mp}$ pairs are produced at a center-of-mass energy of 4.178 GeV. The double tag (DT) method is employed to perform a measurement of the absolute branching fraction. We first select "single tag" (ST) events in which either a D_s^- or D_s^+ meson is fully reconstructed. Then the D_s^+ decay of the interest is searched for in the remainder of each event, namely, in DT events where both the D_s^+ and D_s^- are fully reconstructed, regardless of the γ or π^0 emitted from the $D_s^{*\pm}$ meson. The absolute branching fraction for the D_s^+ meson decay is calculated for each tag mode α and is given by

$$\mathcal{B}^\alpha_{\rm sig} = \frac{N^\alpha_{\rm DT}}{N^\alpha_{\rm ST}\epsilon^\alpha_{\rm DT}/\epsilon^\alpha_{\rm ST}}, \quad (3)$$

where $N^\alpha_{\rm ST}$ and $N^\alpha_{\rm DT}$ are the yields of ST events and DT events, respectively, and $\epsilon^\alpha_{\rm ST}$ and $\epsilon^\alpha_{\rm DT}$ are the ST and DT efficiencies for the tag mode α.

A. ST analysis

All charged tracks must have a polar angle (θ) within $|\cos\theta| < 0.93$, where θ is measured with respect to the direction of the beam. Furthermore, all charged tracks, apart from those from K_S^0 candidates, are required to point back to the interaction point (IP). This is achieved by imposing $V_r < 1$ cm and $|V_z| < 10$ cm, where V_r and $|V_z|$ are the distances of the closest approach to the IP in the transverse plane and along the positron beam direction, respectively. The information from the dE/dx and TOF measurements is combined to evaluate the particle identification (PID) probability ($\mathcal{L}$). A charged track is assigned to be a kaon (pion) candidate if it satisfies $\mathcal{L}_{K(\pi)} > \mathcal{L}_{\pi(K)}$. Candidate K_S^0 mesons are formed from two oppositely charged tracks satisfying $|V_z| < 20$ cm and $|\cos\theta| < 0.93$, which are assumed to be pions without the imposition of further PID requirements. These two tracks are constrained to have a common vertex and the invariant mass of the pair is required to lie within $(0.487, 0.511)$ GeV/c^2. The decay length of the K_S^0 candidates is required to be larger than twice the uncertainty of the decay length.

The D_s^- single-tag candidates are reconstructed in the three tag modes, $K^+K^-\pi^-$, $K_S^0K^-$, and $K_S^0K^+\pi^-\pi^-$, which all have high signal-to-noise ratios and yield the highest sensitivity, according to studies performed on the inclusive MC sample.

To suppress the background involving $D^* \to D\pi$ decays, the momenta of pions from the D_s^- decay are required to be greater than 0.1 GeV/c. The recoil mass evaluated against the D_s^- candidate, $M_{\rm recoil}(D_s^-) = \sqrt{(\sqrt{s} - E_{D_s^-})^2 - |\vec{p}_{D_s^-}|^2}$, is used to reject background from non-$D_s^\pm D_s^{*\mp}$ processes with the requirement that $2.06 < M_{\rm recoil}(D_s^-) < 2.18$GeV/$c^2$. If there are several D_s^- candidates in the event, only that one with recoil mass closest to the D_s^{*+} nominal mass is retained.

An unbinned maximum-likelihood fit is performed on the $M_{D_s^-}$ spectrum of each of the three selected ST tag modes, as shown in Fig. 1. In the fit, the signal shape is taken from the distribution found in MC simulation, using the kernel-estimation method [21] provided as a RooKeysPdf class in ROOT [22], convolved with a Gaussian function. The nonpeaking background is described by a second- or third-order Chebyshev polynomial. The small peaking contribution seen in the $D_s^- \to K_S^0\pi^-$ mode is from $D^- \to K_S^0\pi^-$ decays and its shape is taken from MC simulation, with the absolute normalization determined from the fit.

All the selected D_s^- candidates are retained for further analysis. The resultant yields, $N_{\rm ST}^\alpha$, and the corresponding selection efficiencies $\epsilon_{\rm ST}^\alpha$, as determined from the simulation, are summarized in Table I. The total yield of single tags is $N_{\rm ST}^{\rm tot} = 186091 \pm 719$, where the uncertainty is statistical.

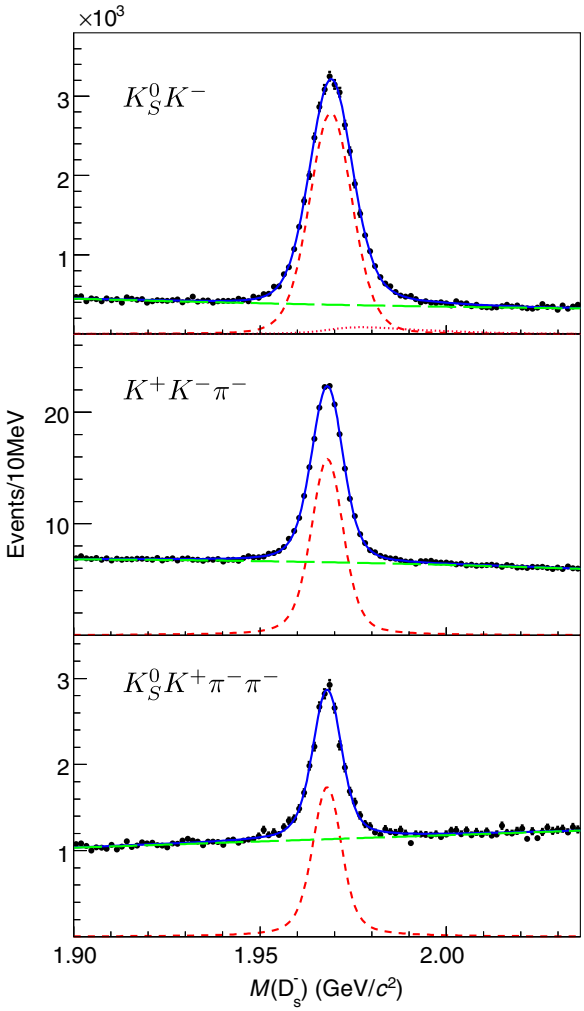

FIG. 1. Fit to the $M_{D_s^-}$ spectrum for each tag mode. The dots with error bars are from the data. The blue solid lines represent the total fit result. The red dashed line and green long-dashed line are the signal shape and nonpeaking background. The pink dotted line in the $K_S^0K^-$ tag mode corresponds to the peak background due to $D^- \to K_S^0\pi^-$.

B. DT analysis

After the reconstruction of the ST D_s^- candidate, there are required to be fewer than four unused charged tracks in the event. We search for proton and electron candidates among these unused tracks. The charged tracks are assigned as proton candidates if they satisfy $\mathcal{L}_p > \mathcal{L}_K$, and $\mathcal{L}_p > \mathcal{L}_\pi$.

TABLE I. Summary of $N_{\rm ST}^\alpha$, $\epsilon_{\rm ST}^\alpha$, and $\epsilon_{\rm DT}^\alpha$ for the tag mode α. All uncertainties are statistical only.

Mode	$N_{\rm ST}^\alpha$	$\epsilon_{\rm ST}^\alpha$ (%)	$\epsilon_{\rm DT}^\alpha$ (%)
$K_S^0K^+$	31267 ± 261	42.32 ± 0.04	8.63 ± 0.07
$K^+K^-\pi^+$	140277 ± 635	49.33 ± 0.18	9.62 ± 0.08
$K_S^0K^-\pi^+\pi^+$	14547 ± 214	21.08 ± 0.07	3.82 ± 0.04

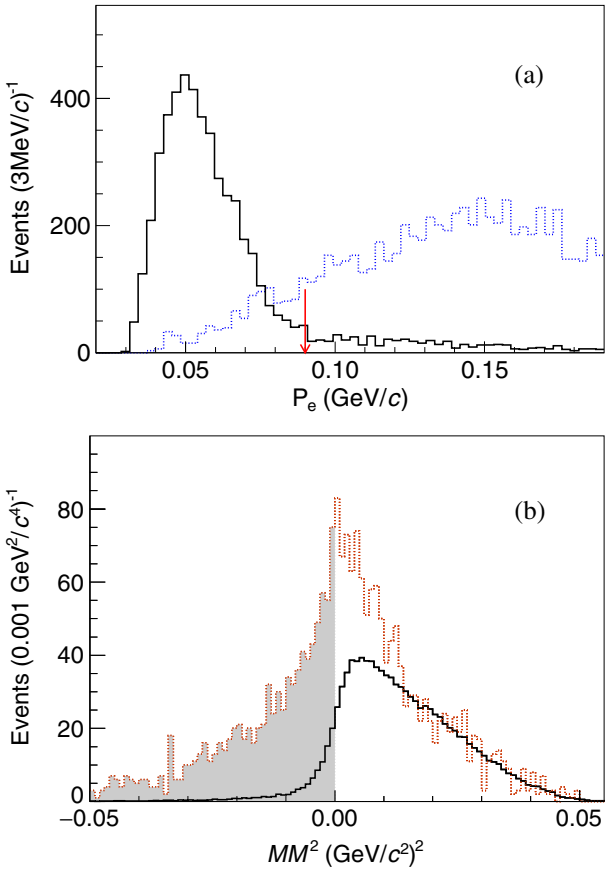

FIG. 2. (a) The electron momentum (P_e) distribution in MC simulation. The green and blue solid histograms represent the signal and background distribution, respectively. The red arrow shows the maximum value of P_e allowed in the selection. (b) The distribution of MM^2 from MC simulation. The red dotted histogram shows the background distribution from the inclusive MC sample, which is completely dominated by the continuum $q\bar{q}$ process. The gray region is rejected by the requirement that $MM^2 > 0$ GeV$^2/c^4$. The solid green histogram shows the signal distribution.

As shown in Fig. 2 the momentum of the electron in the signal decay is typically very low. Consequently, in most decays the electron is not reconstructed in the detector. The presence of the $p\bar{p}$ pair, however, is a sufficiently distinctive signature for such events to be classified as signal, even in the cases when there is no track reconstructed corresponding to the electron. In those cases when a third track is found with lower momentum than the p and $\bar{p}$ candidates, which happens in about 5% of selected events, this track is assigned to be the electron candidate without any PID requirement. Requiring that the momentum of the electron candidate be smaller than 0.09 GeV/c reduces background, whose spectrum is also shown in Fig. 2. The missing mass-squared $MM^2 = (\sqrt{s} - E_{\rm tag} - E_{\rm sig})^2 - (\vec{p}_{\rm tag} + \vec{p}_{\rm sig})^2$ is required to be larger than 0 GeV$^2/c^4$ to further reduce the background from continuum $q\bar{q}$ production, as shown in Fig. 2. Here $E_{\rm tag}$, $\vec{p}_{\rm tag}$ and $E_{\rm sig}$, $\vec{p}_{\rm sig}$ are the total energy and momentum of the tag side and signal side, respectively. As we ignore the momentum of the photon or π^0 from the D_s^* decay, the signal has a predominantly positive value of MM^2 as can be seen in Fig. 2. The DT efficiencies $\epsilon_{\rm DT}^{\alpha}$ as summarized in Table I are determined from simulation and later corrected for the tracking and PID differences between data and MC simulation.

An extended unbinned maximum-likelihood fit to the $M_{D_s^-}$ distribution of the tag meson is used to determine the number of DT signal events. For the tag mode α, the likelihood value is defined as

$$\mathcal{L}^{\alpha} = \frac{e^{-(N^{\alpha}_{\rm sig}+N^{\alpha}_{\rm bkg})}}{n^{\alpha}!} \times \prod_{i=1}^{n^{\alpha}} (N^{\alpha}_{\rm sig}\mathcal{P}^{\alpha}_{\rm sig}(M_{D_s^-}) + N^{\alpha}_{\rm bkg}\mathcal{P}^{\alpha}_{\rm bkg}(M_{D_s^-})), \quad (4)$$

where $n^{\alpha} = N^{\alpha}_{\rm sig} + N^{\alpha}_{\rm bkg}$ is the number of total observed DT events. $N^{\alpha}_{\rm sig}$ and $N^{\alpha}_{\rm bkg}$ denote the fitted yields for signal

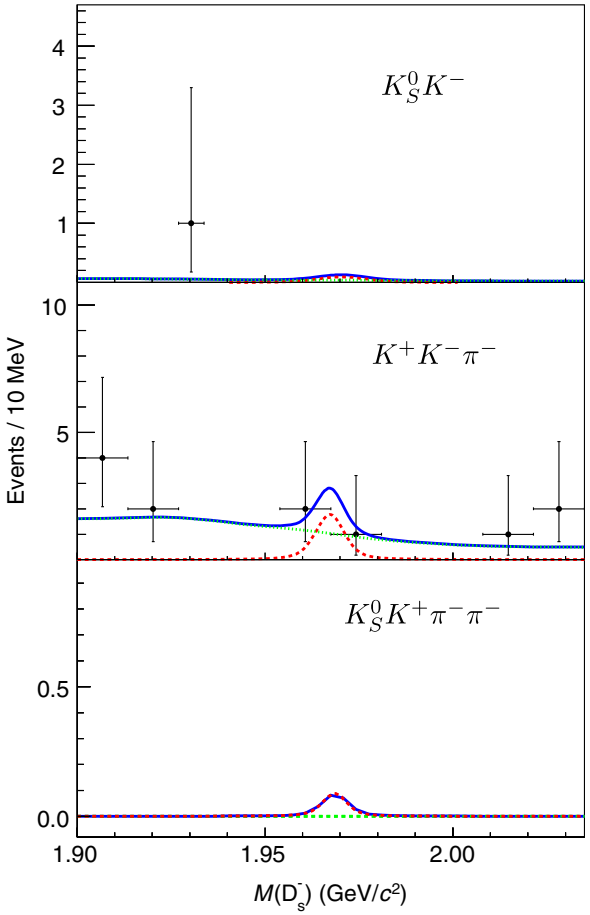

FIG. 3. Fits to $M_{D_s^-}$ after DT event selection. The points with error bars are data, and the blue solid lines show the total fit result. The red and green dotted lines denote the signal and background shapes, respectively.

and backgrounds, respectively, and $\mathcal{P}^{\alpha}_{\rm sig}$ and $\mathcal{P}^{\alpha}_{\rm bkg}$ are the corresponding probability density functions (PDF) in the fit. The PDF distributions are taken from simulation, with the inclusive MC sample being used to represent the background.

A simultaneous fit to the $M_{D_s^-}$ spectra from the three tag modes is performed with the combined likelihood $\mathcal{L}^{\rm com} = \prod_{\alpha=1}^{3} \mathcal{L}^{\alpha}$, sharing the same branching fraction of $D_s^+ \to p\bar{p}e^+\nu_e$ for each.

The fit results are shown in Fig. 3. The signal yields for the three selected ST modes are determined to be $0.3^{+0.4}_{-0.3}$, $1.4^{+1.8}_{-1.3}$, and 0.1 ± 0.1, respectively, and the branching fraction is measured to be $\mathcal{B}(D_s^+ \to p\bar{p}e^+\nu_e) = (0.50^{+0.63}_{-0.44}) \times 10^{-4}$ with a significance of 1.2σ, where the uncertainty is statistical. Since no significant signals are seen, we set an upper limit after taking into account the systematic uncertainties.

IV. SYSTEMATIC UNCERTAINTIES

Possible sources of systematic bias are investigated, and corresponding uncertainties are assigned as discussed below. These uncertainties are listed and added in quadrature in Table II, apart from that component associated with the fit of the DT yields, which is accounted for separately.

A. Fitting ST $M(D_s^-)$ yields

A set of alternative fits is performed, in which the following variations are applied: the background shape is changed from a second- to a third-order Chebyshev polynomial; the signal shape is changed from the MC-simulated shape convolved with a single Gaussian function to the sum of two Gaussian functions; and the fitting range is both increased and decreased by 5 MeV/c^2. The procedures are performed both on inclusive MC and data, and the overall sum in quadrature of the observed differences in the efficiency corrected signal yields is taken as the systematic uncertainty associated with fitting the ST $M_{D_s^-}$ yields.

B. Tracking and PID

The uncertainties associated with the knowledge of the tracking and PID efficiencies for the proton and antiproton are studied with a control sample of $e^+e^- \to p\bar{p}\pi^+\pi^-$ decays. The signal efficiency is reweighted according to the momentum distributions of the proton and antiproton. The uncertainties associated with the tracking and PID efficiencies are assigned to be 2.9% and 2.2%, respectively.

TABLE II. The relative systematic uncertainties (in percent).

Source	Uncertainty
ST yields	0.8
Tracking efficiency	2.9
PID efficiency	2.2
MM^2 requirement	1.0
MC modeling	18
Total	19

C. MM^2 requirement

The systematic uncertainty from the MM^2 requirement is associated with the knowledge of the detector resolution. To estimate this uncertainty a control sample is selected, which has the same tag modes for the D_s^- as in the nominal analysis, and where the other meson is reconstructed in the mode $D_s^+ \to K^+K^-\pi^+$, with the pion then removed and treated as a missing particle. The MM^2 resolution is compared between data and MC simulation, and the difference is applied as additional smearing to the signal MC sample. The difference between the selection efficiencies with this treatment and the nominal analysis is assigned as the systematic uncertainty due to the MM^2 requirement.

D. MC modeling

To estimate the systematic uncertainty due to the possibility of a $p\bar{p}$ bound state, and its assumed mass and width, we simulate and analyze new MC samples that include a resonant system in the decay. We vary the mass of the system from 1.80 to 1.85 GeV/c^2 and the width from 10 to 100 MeV/c^2 [5–7]. The largest relative change of the signal efficiency is found to be 18% and is assigned as the uncertainty from MC modeling.

E. Fitting

It is only necessary to consider the uncertainty on the knowledge of the background shape, as that associated with the signal distribution has negligible impact on the result. The background shape is obtained using the kernel estimation method [21] provided as a RooKeysPdf Class in ROOT [22], based on the inclusive MC sample. Unlike the other sources of uncertainties, the background shape affects the likelihood function directly. We vary the smoothing parameter of RooKeysPdf within a reasonable range to obtain alternative background shapes. We adopt the background shape that gives the largest upper limit on the signal branching ratio to assign the value of this component of the systematic uncertainties.

V. RESULT AND SUMMARY

The upper limit (UL) on the branching fraction is set at the 90% confidence level (CL) according to

$$\frac{\int_0^{\rm UL} L(\mathcal{B})d\mathcal{B}}{\int_0^1 L(\mathcal{B})d\mathcal{B}} = 0.9. \quad (5)$$

Taking the systematic uncertainties (σ_ϵ) into account [23], the likelihood distribution of the branching fraction, $L(\mathcal{B})$, is determined by

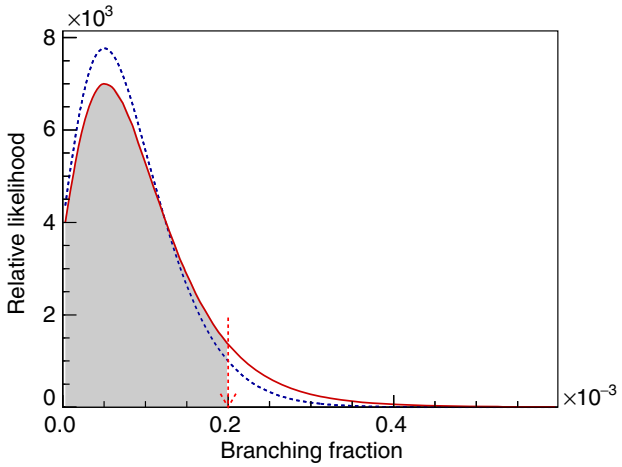

FIG. 4. The likelihood distribution. The blue dotted line denotes the likelihood distribution before the smearing, while the red solid line shows the smeared likelihood.

$$L(\mathcal{B}) \propto \int_0^1 L'\left(\frac{\epsilon}{\epsilon_0}\mathcal{B}\right) e^{-\frac{(\epsilon-\epsilon_0)^2}{2\sigma_\epsilon^2}} d\epsilon, \tag{6}$$

where L' denotes the likelihood of the fit result, ϵ_0 is the nominal signal efficiency based on the signal MC sample, and σ_ϵ is the systematic uncertainty associated with the signal efficiency. The likelihood L' and smeared likelihood L distributions are shown in Fig. 4, and the UL is denoted by the red arrow.

In summary, by analyzing 3.19 fb^{-1} of the e^+e^- annihilation sample collected at $\sqrt{s} = 4.178$ GeV with the BESIII detector, we perform the first search on the decay $D_s^+ \to p\bar{p}e^+\nu_e$, and an upper limit is set at the 90% CL of

$$\mathcal{B}(D_s^+ \to p\bar{p}e^+\nu_e) < 2.0 \times 10^{-4}.$$

In order to improve this limit, and approach the predicted branching ratio of Ref. [4], larger data samples are needed, either at BESIII or at future experiments such as the Belle II experiment [24] and super tau-charm factory [25,26].

ACKNOWLEDGMENTS

The BESIII Collaboration thanks the staff of BEPCII and the IHEP computing center for their strong support. This work is supported in part by National Key Basic Research Program of China under Contract No. 2015CB856700; National Natural Science Foundation of China (NSFC) under Contracts No. 11235011, No. 11875054, No. 11335008, No. 11425524, No. 11625523, No. 11635010, and No. 11935018; the Chinese Academy of Sciences (CAS) Large-Scale Scientific Facility Program; the CAS Center for Excellence in Particle Physics (CCEPP); Joint Large-Scale Scientific Facility Funds of the NSFC and CAS under Contracts No. U1332201, No. U1532257, No. U1532258, and No. U1632107; CAS Key Research Program of Frontier Sciences under Contracts No. QYZDJ-SSW-SLH003 and No. QYZDJ-SSW-SLH040; 100 Talents Program of CAS; National 1000 Talents Program of China; INPAC and Shanghai Key Laboratory for Particle Physics and Cosmology; German Research Foundation DFG under Contracts No. Collaborative Research Center CRC 1044 and No. FOR 2359; Instituto Nazionale di Fisica Nucleare, Italy; Koninklijke Nederlandse Akademie van Wetenschappen (KNAW) under Contract No. 530-4CDP03; Ministry of Development of Turkey under Contract No. DPT2006K-120470; National Natural Science Foundation of China (NSFC) under Contracts No. 11505034 and No. 11575077; National Science and Technology Fund; the Swedish Research Council; U.S. Department of Energy under Contracts No. DE-FG02-05ER41374, No. DE-SC-0010118, No. DE-SC-0010504, and No. DE-SC-0012069; University of Groningen (RuG) and the Helmholtzzentrum fuer Schwerionenforschung GmbH (GSI), Darmstadt; WCU Program of National Research Foundation of Korea under Contract No. R32-2008-000-10155-0.

[1] S. B. Athar *et al.* (CLEO Collaboration), Phys. Rev. Lett. **100**, 181802 (2008).
[2] M. Ablikim *et al.* (BESIII Collaboration), Phys. Rev. D **99**, 031101 (2019).
[3] X. Y. Pham, Phys. Rev. Lett. **45**, 1663 (1980).
[4] H. Y. Cheng and X. W. Kang, Phys. Lett. B **780**, 100 (2018).
[5] J. Z. Bai *et al.* (BES Collaboration), Phys. Rev. Lett. **91**, 022001 (2003).
[6] J. P. Alexander *et al.* (CLEO Collaboration), Phys. Rev. D **82**, 092002 (2010).
[7] M. Ablikim *et al.* (BESIII Collaboration), Phys. Rev. Lett. **108**, 112003 (2012).
[8] S. B. Athar *et al.* (CLEO Collaboration), Phys. Rev. D **73**, 032001 (2006).
[9] M. Ablikim *et al.* (BESIII Collaboration), Phys. Rev. D **87**, 112004 (2013).
[10] M. Ablikim *et al.* (BESIII Collaboration), Phys. Rev. D **93**, 052010 (2016).
[11] D. Scora and N. Isgur, Phys. Rev. D **52**, 2783 (1995).
[12] M. Ablikim *et al.* (BESIII Collaboration), Nucl. Instrum. Methods Phys. Res., Sect. A **614**, 345 (2010).

[13] C. H. Yu *et al.*, *Proceedings of IPAC2016, Busan, Korea* (2016), http://accelconf.web.cern.ch/AccelConf/ipac2016/doi/JACoW-IPAC2016-TUYA01.html.
[14] X. Li *et al.*, Radiat. Detect. Technol. Methods **1**, 13 (2017).
[15] S. S. Li, Y. X. Guo *et al.*, Radiat. Detect. Technol. Methods **1**, 15 (2017).
[16] S. Agostinelli *et al.* (GEANT4 Collaboration), Nucl. Instrum. Methods Phys. Res., Sect. A **506**, 250 (2003).
[17] R. G. Ping, Chin. Phys. C **38**, 083001 (2014).
[18] R. G. Ping, Chin. Phys. C **32**, 243 (2008).
[19] C. Patrignani *et al.* (Particle Data Group), Chin. Phys. C **40**, 100001 (2016).
[20] J. C. Chen, G. S. Huang, X. R. Qi, D. H. Zhang, and Y. S. Zhu, Phys. Rev. D **62**, 034003 (2000); R. L. Yang, R. G. Ping, and H. Chen, Chin. Phys. Lett. **31**, 061301 (2014).
[21] K. S. Cranmer, Comput. Phys. Commun. **136**, 198 (2001).
[22] R. Brun and F. Rademakers, Nucl. Instrum. Methods Phys. Res., Sect. A **389**, 81 (1997).
[23] K. Stenson, arXiv:physics/0605236.
[24] E. Kou *et al.* (Belle-II Collaboration), arXiv:1808.10567.
[25] A. Bondar *et al.* (Charm-Tau Factory Collaboration), Yad. Fiz. **76**, 1132 (2013).
[26] Z. Zhou *et al.*, *7th International Particle Accelerator Conference (IPAC 2016), Busan, Korea* (2016), http://jacow.org/ipac2016/papers/thpor047.pdf.